

GOODS 850-5: A $z > 4$ GALAXY DISCOVERED IN THE SUBMILLIMETER?¹

WEI-HAO WANG,^{2,3} LENNOX L. COWIE,⁴ JENNIFER VAN SADERS,^{3,5} AMY J. BARGER,^{4,6,7} AND JONATHAN P. WILLIAMS⁴

Received 2007 July 22; accepted 2007 October 8; published 2007 October 31

ABSTRACT

We report an SMA interferometric identification of a bright submillimeter source, GOODS 850-5. This source is one of the brightest 850 μm sources in the GOODS-N but is extremely faint at all other wavelengths. It is not detected in the GOODS *HST* ACS images and only shows a weak 2σ signal at 1.4 GHz. It is detected in the *Spitzer* IRAC bands and the MIPS 24 μm band, however, with very low fluxes. We present evidence in the radio, submillimeter, mid-IR, near-IR, and optical that suggest GOODS 850-5 may be a $z > 4$ galaxy.

Subject headings: cosmology: observations — galaxies: evolution — galaxies: formation — galaxies: starburst — infrared: galaxies — submillimeter

1. INTRODUCTION

The Rayleigh-Jeans portion of the dust spectral energy distribution (SED) produces a strong negative K -correction and makes the observed submillimeter flux of a dusty galaxy almost invariant at $z > 1$ to $z \sim 10$ (Blain & Longair 1993). This makes the submillimeter wavelength a potentially powerful probe to the high-redshift universe. However, to date, all the identified submillimeter galaxies are at redshifts lower than 4, likely because of the limited resolution of current submillimeter instruments and the limited sensitivity of current radio instruments.

The Submillimeter Common-User Bolometer Array (SCUBA) on the single-dish James Clerk Maxwell Telescope resolved 20%–30% of the submillimeter extragalactic background light into point sources brighter than ~ 2 mJy at 850 μm (Barger et al. 1999; Eales et al. 1999). Because of the low resolution ($\sim 15''$) of SCUBA, identifications of the submillimeter sources have to assume the radio–far-IR (FIR) correlation in local galaxies (see, e.g., Condon 1992) and rely on radio interferometry to pinpoint the location of the submillimeter emission. Optical spectroscopy of radio-identified submillimeter sources shows that they are ultraluminous ($> 10^{12} L_{\odot}$, corresponding to star formation rates of 10^2 – $10^3 M_{\odot} \text{ yr}^{-1}$) sources at $z \sim 2$ – 3 and that they dominate the total star formation at this redshift (Chapman et al. 2005). However, the positive K -correction of the radio synchrotron emission makes the radio wavelength insensitive to high-redshift galaxies, and radio observations can only identify 60%–70% of the blank-field submillimeter sources (e.g., Barger et al. 2000; Ivison et al. 2002). The radio-unidentified submillimeter sources are commonly thought to be at redshifts higher than the radio detection limit (typically $z \sim 3$ – 4), but there is no direct evidence for such a high-redshift radio-faint submillimeter population.

With recent development in submillimeter interferometry, it is now possible to locate submillimeter sources directly without relying on radio observations. We have begun a program to target radio-faint submillimeter sources with the Submillimeter Array

(SMA)⁸ to determine whether there is a high-redshift ($z > 4$) tail in the redshift distribution of the submillimeter sources. Here we report our first identification in this program, GOODS 850-5. GOODS 850-5 was detected by our SCUBA jiggle-map survey in the Great Observatories Origins Deep Surveys–North (GOODS-N; Giavalisco et al. 2004a) with an 850 μm flux of 12.9 ± 2.1 mJy (Wang et al. 2004). It was also detected in the combined jiggle and scan map of GOODS-N (GN 10; see Pope et al. 2006 and references therein). It is the second brightest submillimeter source in our jiggle-map catalog of the GOODS-N and has an IR luminosity of $\sim 2 \times 10^{13} L_{\odot}$. It does not have a 5σ radio counterpart in the deep Very Large Array (VLA) 1.4 GHz catalogs of Richards (2000) and Biggs & Ivison (2006). We obtained an unambiguous identification of GOODS 850-5 with the SMA and found that the counterpart to this source is remarkably faint at *all* other wavelengths. All data in the optical, near-IR, mid-IR, submillimeter, and radio point to a source at $z > 4$. This is important evidence for the existence of high-redshift submillimeter sources. In this Letter, we report the SMA observation and the multiwavelength photometry (§ 2) and the redshift constraints derived from the photometric data (§ 3). We discuss the implication for the star formation history in § 4 and summarize in § 5. We adopt $H_0 = 71 \text{ km s}^{-1} \text{ Mpc}^{-1}$, $\Omega_{\Lambda} = 0.73$, and $\Omega_M = 0.27$.

2. OBSERVATIONS AND MEASUREMENTS

A full track of SMA observations were obtained on 2007 January 23 using eight antennas in the compact configuration. The receivers were tuned to a frequency of 345.0 GHz centered in the upper sideband, yielding 335.0 GHz in the lower sideband. Each sideband covers a 2 GHz bandwidth and contains 768 spectral channels. The tracking center is at the SCUBA position of GOODS 850-5 ($\alpha[\text{J2000.0}] = 12^{\text{h}}36^{\text{m}}33.45^{\text{s}}$, $\delta[\text{J2000.0}] = 62^{\circ}14'09.43''$). Callisto and the bright quasar 3C 84 were observed to provide flux and bandpass calibrations, respectively. Quasars 1419+543 and 1048+717, respectively 15.5° and 14° away from the target, were observed after every 15 minutes of on-target integration for time-dependent complex gain calibrations. The 225 GHz opacity was an excellent 0.03–0.06, and the dual-sideband system temperature averaged over the entire track was 188 K.

The calibration and data inspection were performed with the Caltech package MIR, modified for the SMA. Continuum data

¹ Based on observations obtained at the Canada-France-Hawaii Telescope (CFHT), which is operated by the National Research Council of Canada, the Institut National des Sciences de l'Univers of the Centre National de la Recherche Scientifique of France, and the University of Hawaii.

² Jansky Fellow; whwang@aoc.nrao.edu.

³ National Radio Astronomy Observatory, Socorro, NM. The NRAO is a facility of the National Science Foundation operated under cooperative agreement by Associated Universities, Inc.

⁴ Institute for Astronomy, University of Hawaii, Honolulu, HI.

⁵ Department of Physics and Astronomy, Rutgers University, Piscataway, NJ.

⁶ Department of Astronomy, University of Wisconsin, Madison, WI.

⁷ Department of Physics and Astronomy, University of Hawaii, Honolulu, HI.

⁸ The Submillimeter Array is a joint project between the Smithsonian Astrophysical Observatory and the Academia Sinica Institute of Astronomy and Astrophysics and is funded by the Smithsonian Institution and the Academia Sinica.

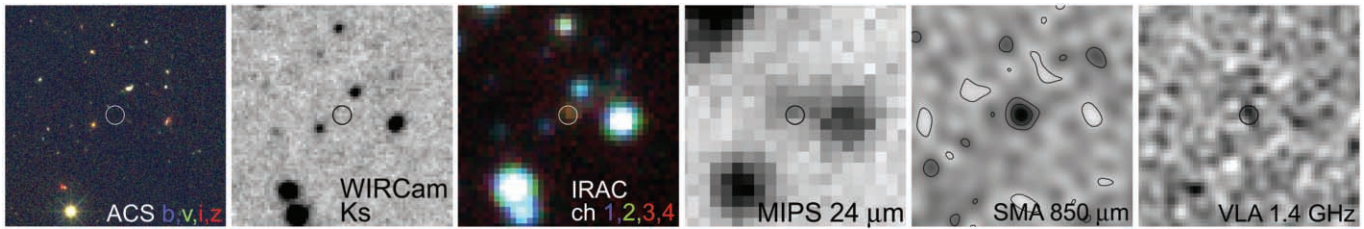


FIG. 1.—Multiwavelength images of GOODS 850-5. Each panel has a size of $24''$. North is up. All four of the ACS (F435W, *b*; F606W, *v*; F775W, *i*; and F850LP, *z*) bands and all four of the IRAC channels (1, 2, 3, and 4) are included in the color pictures. The color codes are labeled in the images. Gray-scale images have inverse scales. The SMA position is labeled with $2''$ diameter circles. The contours in the SMA image have levels of -2 , 2 , 4 , and 6σ , where 1σ is 1.4 mJy beam^{-1} .

were generated by averaging the spectral channels after the pass-band calibration. Both gain calibrators were used to derive gain curves. However, we carried out a separate reduction in which the primary calibrator 1048+717 was used to calibrate 1419+543. The reduced image of 1419+543 has a point source $0.24''$ away from the phase center. Since the two calibrators are separated by a large 28° on the sky, this offset should be only considered as an upper limit to the astrometry error in the reduced image of GOODS 850-5. The calibrated visibility data were Fourier transformed and deconvolved in the package MIRIAD to form images. In the transformation, we weighted each visibility point inversely proportional to the system temperature. Combined with a natural weighting, this provides an optimum signal-to-noise ratio (S/N) and a synthesized beam FWHM of $2.4'' \times 2.2''$ at a position angle of 24° . In the dirty image of GOODS 850-5, a point source is apparent, and we restricted the CLEAN deconvolution to a $\sim 10''$ region centered at the point source. There is no sign of other sources both in the dirty and cleaned images. The noise level in the cleaned image is 1.4 mJy beam^{-1} .

A point source of $12.0 \pm 1.4\text{ mJy}$ is clearly detected very close to the phase center. A Gaussian fit to the image yields a source profile identical to the synthesized beam, indicating an unresolved source with good calibrations. The fit provides a source position of $\alpha(\text{J2000.0}) = 12^{\text{h}}36^{\text{m}}33.45^{\text{s}}$, $\delta(\text{J2000.0}) = 62^\circ14'08.65''$, which agrees extremely well with the SCUBA position. The positional error in the fit is $0.2''$, consistent with the angular resolution for this S/N and also comparable to the aforementioned upper limit to the astrometry error derived from the calibrator 1419+543. We also performed a point-source fit

directly to the visibility data, and the result is fully consistent with the fit in the image plane.

We present the GOODS *Hubble Space Telescope* (HST) Advanced Camera for Surveys (ACS) images (Giavalisco et al. 2004a), our CFHT WIRCam K_s -band image (36 hr of integration; R. C. Keenan et al. 2008, in preparation), the GOODS *Spitzer* Legacy Program (M. Dickinson et al. 2008, in preparation) Infrared Array Camera (IRAC) and Multiband Imaging Photometer for *Spitzer* (MIPS) images, the VLA image (Biggs & Ivison 2006), and our SMA image of GOODS 850-5 in Figure 1. In all of the four ACS images (F435W, F606W, F775W, and F850LP) and the WIRCam image, there are no galaxies within $0.5''$ from the SMA position. A faint galaxy is clearly detected by *Spitzer* in all four IRAC bands and in the $24\ \mu\text{m}$ MIPS band right at the SMA position. Because of the high accuracy ($0.2''$) of the SMA astrometry, this *Spitzer* source is a robust identification of GOODS 850-5. We list our broadband fluxes in Table 1. The $850\ \mu\text{m}$ flux is a noise-weighted mean from the SCUBA jiggle map (Wang et al. 2004) and the SMA measurement. Typical errors in flux calibrations at this wavelength are $\geq 10\%$ and could be larger than the noise. However, the fact that the SMA flux and the SCUBA flux agree with each other extremely well suggests good flux calibrations in both experiments. The 1.4 GHz flux is measured at the SMA position from the VLA image of Biggs & Ivison (2006) assuming a point source and with a primary beam correction. The ACS and WIRCam fluxes are also measured at the SMA position with, respectively, $0.8''$ and $1.5''$ diameter apertures. Measuring fluxes in the *Spitzer* bands is more difficult. In the 3.6 and $4.5\ \mu\text{m}$ images, there is a nearby blue galaxy blended with GOODS 850-5. There is another galaxy blended with GOODS 850-5 in the MIPS image. To deconvolve the fluxes, we performed point-spread function (PSF) fitting to the blended sources. We used the IRAC and MIPS in-flight PSFs and applied simultaneous two-component fits to the two sources, and scaled the measured fluxes to total fluxes using the PSFs. To verify the fluxes measured in this way, we first compared them with simple aperture-corrected aperture fluxes. We found that at 5.8 and $8.0\ \mu\text{m}$ where GOODS 850-5 is isolated, the PSF fitting provides fluxes consistent with the aperture fluxes. We also used the SExtractor package (Bertin & Arnouts 1996) to measure fluxes. SExtractor could deblend the two sources at $4.5\ \mu\text{m}$ but not at $3.6\ \mu\text{m}$ even with the most aggressive deblending. The aperture-corrected SExtractor fluxes at $4.5\ \mu\text{m}$ and longer are all consistent with the PSF fitting fluxes. We thus conclude that our PSF fitting provides reliable estimates of the fluxes of GOODS 850-5. The *Spitzer* fluxes listed in Table 1 are all measured with the PSF fitting method.

We note that our SMA identification confirms the counterpart suggested by Pope et al. (2006). Our carefully measured *Spitzer* fluxes are also consistent with the SExtractor pipeline fluxes

TABLE 1
PHOTOMETRY OF GOODS 850-5

Wave Band	Flux (μJy)
F435W	-0.013 ± 0.004
F606W	-0.004 ± 0.003
F775W	0.001 ± 0.006
F850LP	-0.009 ± 0.009
K_s	0.055 ± 0.052
$3.6\ \mu\text{m}$	1.14 ± 0.14
$4.5\ \mu\text{m}$	1.64 ± 0.13
$5.8\ \mu\text{m}$	2.33 ± 0.24
$8.0\ \mu\text{m}$	5.37 ± 0.37
$24\ \mu\text{m}$	46.3 ± 9.2
$850\ \mu\text{m}$	12300 ± 1200
1.4 GHz	18.7 ± 8.0

NOTE.—The conversion between microjanskys and AB magnitude is $\text{AB} = 23.9 - 2.5 \log(\mu\text{Jy})$.

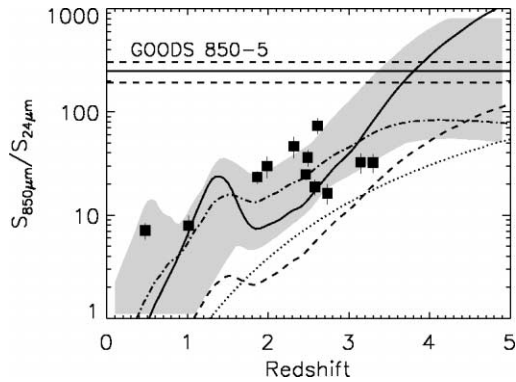


FIG. 2.— $S_{850\mu\text{m}}/S_{24\mu\text{m}}$ flux ratio vs. redshift. Curves are filter-convolved Silva et al. (1998) model SEDs of Arp 220 (ultraluminous starburst: *solid curve*), M100 (normal spiral: *dash-dotted curve*), and M82 (low-luminosity starburst: *dashed curve*), and Mrk 231 (ultraluminous dusty AGN: *dotted curve*) derived from the photometry in NED. The shaded region is the range of the models in Chary & Elbaz (2001). Filled squares are GOODS-N SCUBA sources identified at $24\mu\text{m}$ or 1.4GHz (Wang et al. 2006). Horizontal lines are GOODS 850-5 and the 1σ error.

in Pope et al. The 1.4GHz flux in Pope et al. is 76% larger than ours, but the difference is within the errors.

3. REDSHIFT CONSTRAINTS

GOODS 850-5, one of the brightest $850\mu\text{m}$ sources in the GOODS-N, is incredibly faint at *all* other wavelengths. Because of the optical and near-IR faintness, it is difficult to obtain its redshift through spectroscopy. We obtained redshift constraints for GOODS 850-5 using the multiwavelength broadband fluxes. There are three independent pieces of evidence that suggest GOODS 850-5 is a $z > 4$ galaxy.

By assuming that the well-known radio-FIR correlation for local star-forming galaxies also applies to submillimeter sources, we can estimate the redshift using the radio and submillimeter fluxes (e.g., Carilli & Yun 1999; Barger et al. 2000). Barger et al. assumed pure power-law SEDs in both the radio and the submillimeter and obtained the formula $z = 0.98(S_{850\mu\text{m}}/S_{1.4\text{GHz}})^{0.26} - 1$, based on Arp 220. This implies $z \sim 4.3$ for GOODS 850-5. This is a lower limit, because the peak of the dust SED and the free-free emission start to move in the observed bands at $z > 4$. Both effects underestimate the redshift. By adopting the complete Arp 220 SED model in Silva et al. (1998), we find $z \sim 5.6$ for GOODS 850-5 ($z \sim 4.3$ if we adopt the radio flux of $33.1\mu\text{Jy}$ in Pope et al. 2006). This redshift estimate is nevertheless very crude. Because of the uncertainties in the submillimeter and radio SEDs and the radio-FIR correlation at high redshift, such redshift estimates typically have an error of ± 0.5 (e.g., Ivison et al. 2002).

The unusually large $S_{850\mu\text{m}}/S_{24\mu\text{m}}$ ratio also suggests a high redshift of $z > 3$. As can be seen in Figure 2, the $S_{850\mu\text{m}}/S_{24\mu\text{m}}$ ratio of GOODS 850-5 is an order of magnitude higher than the mean value for other identified submillimeter sources in the GOODS-N. This can only be explained by a $z > 3$ galaxy with any dust SEDs allowed by current models.

Finally, we used the photometric redshift technique to test if the *HST*, *WIRCam*, and *Spitzer* SED of GOODS 850-5 can be fitted with a $z > 4$ galaxy. Because there is not a unique correlation between the dust SED and stellar SED of galaxies, we only included the ACS, *WIRCam*, and IRAC passbands in the photometric redshift study to account for just the stellar emission. Although GOODS 850-5 is not detected in the ACS images, the upper limits to the ACS fluxes suggest a very red SED at $< 3\mu\text{m}$ (Fig. 3) and thus still provide useful constraints.

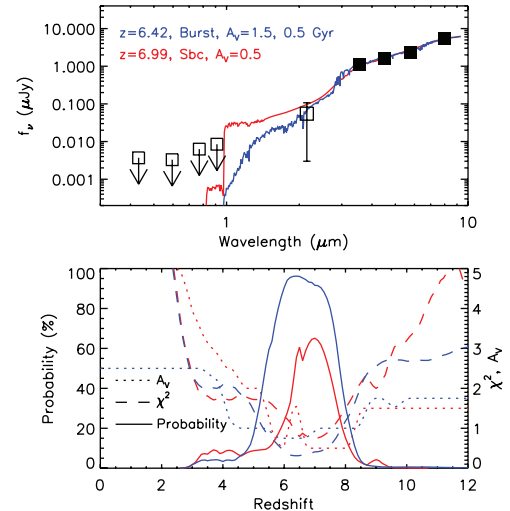


FIG. 3.—Photometric redshift result for GOODS 850-5. The upper panel shows the observed IRAC, *WIRCam*, and ACS SEDs (*squares*) and the best-fit SEDs (*solid curves*) in the empirical set (*red*) and in the population synthesis set (*blue*). The lower panel shows the χ^2 (*dashed curves*), the corresponding probability (*solid curves*), and the extinction (*dotted curves*) of the best-fit SEDs vs. redshift for the two SED sets (same color coding as in the upper panel).

In the photometric redshift fitting, we assigned zeros to the ACS fluxes and used the 1σ errors as the flux uncertainties. We used the measured K_s flux, even though it is only 1σ .

We used the popular Hyperz package (Bolzonella et al. 2000). We limited the redshift range to $z = 0-12$ and adopted the Calzetti et al. (2000) extinction of $A_V = 0-5$. We used two sets of SEDs. The first set consists of empirically observed SEDs, including the Im, Scd, Sbc, and E type galaxies in Coleman et al. (1980) and the starburst SEDs SB2 and SB3 in Kinney et al. (1996). The primary solution provided by Hyperz is $z = 6.99$, $A_V = 0.5$, and a Sbc type galaxy. The corresponding probability is 65.1%, and the 99% confidence range is $z = 5.6-8.0$. The second SED set is the stellar population synthesis models included in Hyperz, which is based on the earlier version of Bruzual & Charlot (1993). The primary solution is $z = 6.42$, $A_V = 1.5$, and a burst-type SED with an age of 0.5 Gyr. The corresponding probability is 96.4%, and the 99% confidence range is $z = 5.2-8.0$. In both SED sets, the photometric redshift confidence range is consistent with the range allowed by the radio, submillimeter, and mid-IR flux ratios discussed above. In Figure 3, we show the fitted and observed SEDs, and the best-fit χ^2 , probability, and extinction as functions of redshift. The SED can only be fitted with $A_V > 2$ at $z < 3$, and the probabilities at $z < 3$ of the best-fit models are zero even when $A_V = 10$ is allowed in the fitting. Therefore, a highly reddened galaxy at $z < 3$ is ruled out for GOODS 850-5. In the photometric redshift fitting, an intermediate redshift of $3-4.5$ is not entirely ruled out, although the probability is low ($< 10\%$).

The primary uncertainty in the above analyses is the possibility of the existence of an active galactic nucleus (AGN), whose SED may be different than the ones used for the radio, submillimeter, IR, and optical photometric analyses. We argue that whether or not there is an AGN is not likely to change the high redshift of GOODS 850-5. First, GOODS 850-5 is not detected in the 2 Ms *Chandra* images (Alexander et al. 2003) in either the hard or soft X-ray bands. This rules out a Compton-thin AGN at $z < 3$. (The 2 Ms *Chandra* observations can detect a 10^{42} and $10^{42.5}$ ergs s^{-1} soft and hard X-ray source, respectively, at $z \sim 3$.) The best ex-

ample of a local Compton-thick AGN in the far-IR luminosity class of GOODS 850-5 is Mrk 231. Although the IRAC power-law spectral slope of GOODS 850-5 is similar to that of Mrk 231, its $S_{850\ \mu\text{m}}/S_{24\ \mu\text{m}}$ flux ratio is more than an order of magnitude higher than Mrk 231 at $z < 3$ (Fig. 2⁹); i.e., GOODS 850-5 does not show much of the warm dust emission that is characteristic for a heavily obscured AGN. Furthermore, the rest-frame 1.4 GHz flux of Mrk 231 also follows the radio-FIR correlation for normal galaxies with a q -value of 2.24 (under the definition of q in Condon 1992), but it has a flat radio spectrum (a smaller K -correction in the radio). Therefore, even if GOODS 850-5 is an AGN that is similar to Mrk 231, its large $S_{850\ \mu\text{m}}/S_{1.4\ \text{GHz}}$ flux ratio will suggest a redshift even higher than that estimated from the Arp 220 template.

4. IMPLICATIONS FOR THE STAR FORMATION HISTORY

There is growing evidence for a significant submillimeter population at $z > 4$. Dunlop et al. (2004) presented evidence for an optically faint $z \sim 4.1$ galaxy for HDF 850.1. More recent SMA results of Younger et al. (2007) suggest a number of radio and optically faint submillimeter sources to be at $z \gtrsim 4$. GOODS 850-5 is similar to these galaxies. On the other hand, GOODS 850-5 has the highest $S_{850\ \mu\text{m}}/S_{1.4\ \text{GHz}}$ flux ratio and also has higher quality data at many other wavelengths. Unlike HDF 850.1, which is behind a bright galaxy, GOODS 850-5 can be studied in detail especially in the optical and IR wavelengths.

The discovery of GOODS 850-5 and its like extends the redshift distribution of bright submillimeter sources to beyond 4.0 and perhaps even to $z > 5$. The 12.3 mJy 850 μm flux of GOODS 850-5 implies an IR luminosity of $\sim 2.3 \times 10^{13} L_{\odot}$ ($L_{\text{IR}} = 1.9 \times 10^{12} S_{850\ \mu\text{m}} L_{\odot} \text{mJy}^{-1}$; Blain et al. 2002) and therefore a very high star formation rate of $\sim 4000 M_{\odot} \text{yr}^{-1}$ ($\dot{M} = 1.7 \times 10^{-10} L_{\text{IR}}/L_{\odot}$; Kennicutt 1998). This is an extraordinary amount of star formation at high redshift, but it can only be identified in the submillimeter. Even if such a source could be picked up in optical and near-IR broadband dropout surveys, its star formation would still be missed due to the extreme faintness in the rest-frame UV. How much can hidden sources like this affect the current picture of the cosmic star formation history at high redshift?

Bright submillimeter sources (> 2 mJy at 850 μm) contribute

⁹ The NASA/IPAC Extragalactic Database (NED) is operated by the Jet Propulsion Laboratory, California Institute of Technology, under contract with the National Aeronautics and Space Administration.

$\sim 10 \text{ Jy deg}^{-2}$ to the total background, and 60%–70% of them have radio counterparts. We assume that all of the $\sim 4 \text{ Jy deg}^{-2}$ radio-identified bright submillimeter sources are at $z = 4$ –7. With the above conversions between 850 μm flux, IR luminosity, and star formation rate, this implies a mean comoving IR luminosity density of $\sim 2.2 \times 10^8 L_{\odot} \text{Mpc}^{-3}$ and therefore a star formation rate density (SFRD) of $\sim 0.04 M_{\odot} \text{yr}^{-1} \text{Mpc}^{-3}$. This is consistent with the estimate in Barger et al. (2000) based on a smaller sample of radio-identified submillimeter sources, after taking into account the differences in cosmology. Our value of $0.04 M_{\odot} \text{yr}^{-1} \text{Mpc}^{-3}$ averaged over $z = 4$ –7 is ~ 2 times higher than the typical value of 0.01–0.02 $M_{\odot} \text{yr}^{-1} \text{Mpc}^{-3}$ at $z \sim 4$ determined from optical surveys without extinction correction (e.g., Giavalisco et al. 2004b; Bouwens et al. 2003). In general, Lyman break galaxies are not bright submillimeter sources (Peacock et al. 2000; Chapman et al. 2000; Webb et al. 2003), suggesting that most (if not all) of the above SFRD estimated from the radio-identified bright submillimeter sources is missed by optical surveys. Although our SFRD of $0.04 M_{\odot} \text{yr}^{-1} \text{Mpc}^{-3}$ is likely an upper limit due to the assumptions, it still shows the significance of dust-hidden star formation at high redshift.

5. SUMMARY

We obtained accurate astrometry for the bright submillimeter source GOODS 850-5 with the SMA interferometer at 850 μm . The counterpart is extremely faint in the optical, near-IR, mid-IR, and radio. Both the radio and 24 μm faintness of GOODS 850-5 suggests a high redshift of $z > 4$. The very red SED between 3.6 and 8.0 μm and the nondetection in the optical and K_s bands can only be fitted by stellar continuum at $z > 4$. This discovery provides important evidence that some of the radio-undetected submillimeter sources are at high redshift and extends the redshift distribution of bright submillimeter sources to $z > 4$. It suggests that a great fraction of star formation at high redshift is hidden from optical surveys.

We thank L. Silva and R. Chary for providing the SED templates, the SMA staff for the help on observation and data reduction, and the referee for the comments that greatly improved the manuscript. We gratefully acknowledge support from NRAO (W.-H. W.), NRAO REU program (J. v. S.), NSF grants AST 04-07374 (L. L. C.) and AST 02-39425 (A. J. B.), the University of Wisconsin Research Committee with funds granted by the Wisconsin Alumni Research Foundation, and the David and Lucile Packard Foundation (A. J. B.).

REFERENCES

- Alexander, D. M., et al. 2003, *AJ*, 126, 539
 Barger, A. J., Cowie, L. L., & Richards, E. A. 2000, *AJ*, 119, 2092
 Barger, A. J., Cowie, L. L., & Sanders, D. B. 1999, *ApJ*, 518, L5
 Bertin, E., & Arnouts, S. 1996, *A&AS*, 117, 393
 Biggs, A. D., & Ivison, R. J. 2006, *MNRAS*, 371, 963
 Blain, A. W., & Longair, M. S. 1993, *MNRAS*, 264, 509
 Blain, A. W., Smail, I., Ivison, R. J., Kneib, J.-P., & Frayer, D. T. 2002, *Phys. Rep.*, 369, 111
 Bolzonella, M., Miralles, J.-M., & Pelló, R. 2000, *A&A*, 363, 476
 Bouwens, R., Broadhurst, T., & Illingworth, G. 2003, *ApJ*, 593, 640
 Bruzual, G., & Charlot, S. 1993, *ApJ*, 405, 538
 Calzetti, D., Armus, L., Bohlin, R. C., Kinney, A. L., Koornneef, J., & Storchi-Bergmann, T. 2000, *ApJ*, 533, 682
 Carilli, C. L., & Yun, M. S. 1999, *ApJ*, 513, L13
 Chapman, S. C., Blain, A. W., Smail, I., & Ivison, R. J. 2005, *ApJ*, 622, 772
 Chapman, S. C., et al. 2000, *MNRAS*, 319, 318
 Chary, R., & Elbaz, D. 2001, *ApJ*, 556, 562
 Coleman, G. D., Wu, C.-C., & Weedman, D. W. 1980, *ApJS*, 43, 393
 Condon, J. J. 1992, *ARA&A*, 30, 575
 Dunlop, J. S., et al. 2004, *MNRAS*, 350, 769
 Eales, S., Lilly, S., Gear, W., Dunne, L., Bond, J. R., Hammer, F., Fèvre, O. L., & Crampton, D. 1999, *ApJ*, 515, 518
 Giavalisco, M., et al. 2004a, *ApJ*, 600, L93
 ———. 2004b, *ApJ*, 600, L103
 Ivison, R. J., et al. 2002, *MNRAS*, 337, 1
 Kennicutt, R. C., Jr. 1998, *ARA&A*, 36, 189
 Kinney, A. L., Calzetti, D., Bohlin, R. C., McQuade, K., Storchi-Bergmann, T., & Schmitt, H. R. 1996, *ApJ*, 467, 38
 Peacock, J. A., et al. 2000, *MNRAS*, 318, 535
 Pope, A., et al. 2006, *MNRAS*, 370, 1185
 Richards, E. A. 2000, *ApJ*, 533, 611
 Silva, L., Granato, G. L., Bressan, A., & Danese, L. 1998, *ApJ*, 509, 103
 Wang, W.-H., Cowie, L. L., & Barger, A. J. 2004, *ApJ*, 613, 655
 ———. 2006, *ApJ*, 647, 74
 Webb, T. M., et al. 2003, *ApJ*, 582, 6
 Younger, J. D., et al. 2007, *ApJ*, in press (arXiv: 0708.1020)